



Simulations on the prediction of cod (*Gadus morhua*) freshness from an intelligent packaging sensor concept

Heising, J. K., van Boekel, M. A. J. S., & Dekker, M.

This is a "Post-Print" accepted manuscript, which has been published in "Food Packaging and Shelf Life"

This version is distributed under a non-commercial no derivatives Creative Commons



([CC-BY-NC-ND](https://creativecommons.org/licenses/by-nc-nd/4.0/)) user license, which permits use, distribution, and reproduction in any medium, provided the original work is properly cited and not used for commercial purposes. Further, the restriction applies that if you remix, transform, or build upon the material, you may not distribute the modified material.

Please cite this publication as follows:

Heising, J. K., van Boekel, M. A. J. S., & Dekker, M. (2015). Simulations on the prediction of cod (*Gadus morhua*) freshness from an intelligent packaging sensor concept. *Food Packaging and Shelf Life*, 3, 47-55.
<https://doi.org/10.1016/j.fpsl.2014.10.002>

1 **Simulations on the prediction of cod (*Gadus morhua*) freshness from**
2 **an intelligent packaging sensor concept.**

3

4

5

6 J. K. Heising^a, M. A. J. S. van Boekel^a and M. Dekker^{a*}

7

8 ^a Food Quality and Design Group, Department of Agrotechnology and Food Sciences,
9 Wageningen University, P.O. Box 17, 6700 AA Wageningen, The Netherlands

10

11

12

13

14

15

16

17

18

19

20 * Correspondence to M. Dekker, Food Quality and Design Group, Department of
21 Agrotechnology and Food Sciences, P.O. Box 17, 6700 AA Wageningen, The
22 Netherlands.

23 +31 317 483214

24 E-mail: Matthijs.Dekker@wur.nl

25

26 **Abstract**

27 A non-destructive method that monitors changes in the freshness status of packed cod
28 fillets has potential for the development of an intelligent packaging concept. The
29 method is based on monitoring volatile compounds that dissolve and dissociate in the
30 sensing aqueous phase. A mathematical model was developed to predict the freshness
31 of the packed fish from the sensor signal (based on trimethylamine (TMA)). The
32 model is based on physical and (bio)chemical principles of biological formation, mass
33 transport, partitioning, and dissociation of TMA. The parameters in the model are
34 derived partly from physical chemical properties, partly estimated from fitting the
35 non-destructive sensor measurements in the aqueous phase and destructive TMA
36 measurements in cod fillets. The model predicts a TMA increase in the aqueous phase
37 comparable with sensor measurements from experimental storage trials. The initial
38 freshness of fish is variable and taken into account in the model in the predictions of
39 the freshness status of the packed fish.

40 The model was used to test different scenarios for sensor design. This showed clearly
41 that minimizing the aqueous phase will strongly improve the sensitivity of the sensor.
42 Reducing the package headspace can further improve the sensitivity.

43 In conclusion, the model can make accurate freshness predictions at a constant
44 temperature of 0 °C and also in case of temporally temperature abuse, but needs a
45 temperature-dependent correction for higher temperatures. Therefore combining the
46 conductivity-sensor with a temperature sensor enables this model to be used in the
47 development of an intelligent packaging to monitor the freshness of fish.

48

49

50 **Keywords**

51 Mathematical modelling, trimethylamine (TMA), fish freshness, dynamic models,
52 temperature effect, intelligent packaging sensor

53

54 **1. Introduction**

55 Dynamic information about the quality status of foods supplied by intelligent
56 packaging can contribute substantially to the optimization of supply chain
57 management (Realini & Marcos, 2014). Intelligent packaging for foods requires the
58 development of sensors that monitor and communicate freshness from the moment of
59 packaging until the day the fish is spoiled (Kuswandi et al., 2011). Foods like fresh
60 fish, with a highly variable quality on the moment of packaging, require sensors
61 monitoring compounds directly correlated with food quality (Heising, Dekker,
62 Bartels, & Van Boekel, 2014b). Freshness is a very important factor determining the
63 quality of fish and freshness can be evaluated by different approaches, e.g. from
64 analysis of volatiles (Ólafsdóttir et al., 1997).

65 An intelligent packaging sensor concept that consists of a non-destructive method to
66 monitor changes in the freshness of packed cod fillets has been introduced in a
67 previous study (Heising, Dekker, Bartels, & Van Boekel, 2012). The principle of this
68 method is the introduction of an aqueous phase in the headspace of the fish package.
69 In this aqueous phase, changes in the electrical properties can be monitored by
70 electrodes, e.g. by using a conductivity electrode (Heising, Bartels, Van Boekel, &
71 Dekker, 2014a). The changes in the electrical properties of the aqueous phase were
72 related to the total volatile basic nitrogen content (TVB-N) of the fish itself, which has
73 proven to be a good indicator for the freshness of many marine fish (Botta, Lauder, &
74 Jewer, 1984).

75 The increase in the TVB-N content is mainly caused by the formation of
76 trimethylamine (TMA) in fish, the compound that is one of the dominant components
77 of spoiling fish and that has a typical fishy odour (Huss, 1995; Howgate, 2010). The
78 TMA content is strongly correlated to the sensory quality of cod (Burt, Gibson, Jason,
79 & Sanders, 1976; Gill, 1990).

80 In this article, we describe the framework for a mathematical model to predict the
81 sensor response of the intelligent packaging concept from the TMA content in the
82 aqueous phase inside a fish package. The model was fitted on data of the electrode
83 response measured during a trial when fish was stored at 15 °C. Furthermore,
84 simulations were conducted using the model with changes in the parameters in order
85 to predict the sensor response on miniaturization, a necessary step in the further
86 development of the intelligent packaging concept (Vanderroost, Ragaert, Devlieghere,
87 & De Meulenaer, 2014).

88 In a previous publication models for TMA formation were developed, based on
89 microbial growth models (Heising, Van Boekel, & Dekker, 2014c). The aim of this
90 research is to develop a mathematical model, based on physical and biochemical
91 principles of mass transport, to translate the sensor signal of an intelligent packaging
92 concept into a prediction of fish freshness and to simulate the miniaturized intelligent
93 packaging concept.

94

95 **2. Materials and Methods**

96

97 **2.1 Data collection**

98

99 *2.1.1 Storage trial of cod fillets*

100 Data for parameter estimation were collected in the experimental trials with cod fillets
101 stored at 0-15 °C as described by Heising et al. (2014a),.

102 Cod (*Gadus morhua*) was bought at a wholesale in IJmuiden (NL) in May 2008. The
103 cod was caught in the North Sea off the Netherlands, gutted on board the fishing
104 vessels, stored on ice and brought to IJmuiden. After the auction, the wholesaler
105 prepared skinned fillets from the cod and the fillets were transported on ice to the
106 laboratory in ~3 hours. Purchase, fillet preparation and transport all took place the
107 same morning. Immediately after arriving in Wageningen, the fillets were prepared
108 for analysis and storage, and from this moment the storage trial started. The batch of
109 fish was used for both the non-destructive and destructive analysis during the trial.

110

111 *2.1.2 Non-destructive method*

112 The non-destructive measurement setup consisted of a glass-cell with holes in the lid
113 for air tight fitting of the electrodes to analyze an aqueous phase in a beaker separate
114 from the fish (Figure 1) (Heising et al., 2012).

115 Cod fillets (~375 g) sliced into pieces of approximately 30 g, were put in the glass
116 cell. Each experiment contained randomly mixed pieces from different cod fillets. The
117 glass cell contained a conductivity electrode (TetraCon 325 conductivity electrode
118 with inoLab Cond 730 precision conductivity meter, WTW) with the electrode-tip in
119 65 ml Milli-Q (deionized) water in the beaker. The conductivity electrode was logged
120 automatically at time-intervals of 15 minutes.

121 The glass cells were placed in a cryostat set at temperatures from 0 till 15 °C, filled
122 with water and antifreeze, located in a room that was temperature controlled.

123

124 *2.1.3 Destructive TMA analysis*

125 The fish samples for the destructive TMA analysis were packed separately in
126 aluminum boxes, one box for each measurement day. After arrival in Wageningen, the
127 fillets were sliced into pieces of approximately 30 g, the pieces were mixed and 120 g
128 fish was put into each box with a lid for storage. The boxes were stored in a
129 refrigerator at temperatures from 0 till 15 °C. The temperature of the fillets and the
130 storage rooms was monitored with Automatic wireless temperature loggers as
131 described in Heising et al. (2012).

132 The TMA content was determined in duplicate in an extract of the cod fillet according
133 to the steam distillation method from Malle & Tao (1987) as described in Heising et
134 al. (2012). 20 ml of ~36% aqueous formaldehyde-solution (Fluka 47630)
135 (formaldehyde complexes with primary and secondary amines, but not with tertiary
136 amine TMA) was added to 25 ml of filtrate, followed by 5 ml of 10% (w/v) NaOH.
137 Steam distillation (Gerhard Vadopest 12-Kjedahl type distillatory) was carried out for
138 7.3 minutes on the TCA extract. A beaker containing 10 ml of a 4% aqueous boric
139 acid solution (Merck 1.00165) and 0.04 ml of Mixed indicator 5 for ammonia
140 titrations (Merck 1.06130) was placed at the end of the condenser. The boric acid
141 solution turned green when alkalinized by the distilled TMA. The green alkaline
142 distillate was titrated using a digital burette (Schott type T80 /20) containing an
143 aqueous 0.1N hydrochloric acid solution (Merck 1.09973). Complete neutralization
144 was obtained when the colour turned pink on the addition of a further drop of
145 hydrochloric acid. This procedure was repeated for duplicate analysis.

146

147 **2.2 Parameter estimation and simulations**

148

149 The mass transfer of TMA in packed cod fillets was modelled using sets of algebraic
150 and differential equations. Simulations and parameter estimation from numerical
151 integration of the differential equations, including the statistical evaluation of the
152 parameters and performance of the complete model, were obtained by least squares
153 regression with the help of the software package Athena Visual Workbench (Stewart
154 et al., 1992; www.athenavisual.com).

155

156

157 **3. Results and Discussion**

158

159 **3.1 Model development**

160

161 The modelling approach is based on the formation of volatile compounds. In freshly
162 caught cod the volatile NH_3 and some other volatile compounds are present. During
163 subsequent storage the content of volatiles increases, mainly due to the formation of
164 TMA. In a later stage, when the fish is already spoiled, NH_3 is increasing further. This
165 formation of volatiles can be linked to the freshness and quality of fish (Ólafsdóttir et
166 al., 1997). We realize that quality is a broad concept and the combined analysis of
167 several quality attributes (e.g. protein and fat degradation, microbial growth and
168 sensory aspects) could lead to more accurate description of the quality status.
169 However for the development of a sensor a non-destructive approach is required.
170 Volatiles can be measured non-destructively. The TMA content is a good indicator
171 since it is correlated to the freshness status and also other quality attributes (Burt et
172 al., 1976).

173

174 The non-destructive method consists of an aqueous phase in which electrodes measure
175 the changes in the electrical properties of the aqueous phase (Figure 1). These changes
176 are caused by volatiles produced by the packed fish fillet, that will partition in the
177 headspace and dissolve in the aqueous phase.

178

179 3.1.1 Formation of TMA

180 TMA is produced on fresh cod fillets stored at chilled and higher temperatures (in the
181 range 0-15 °C) by the micro-organisms *Shewanella putrefaciens* and *Photobacterium*
182 *phosphoreum* and the formation can be described by a dynamic model (Heising et al.,
183 2014c):

$$184 \quad \frac{dC_{TMA}}{dt} = \mu_{max} C_{TMA} \left(1 - \left(\frac{C_{TMA}}{C_{max}} \right) \right) \quad (1)$$

185

186 With:

187 C_{TMA} concentration of TMA at time t (mg TMA-N per 100 g fish)

188 t time (hours)

189 C_{max} upper asymptote concentration (mg TMA-N per 100 g fish)

190 μ_{max} maximum specific formation rate coefficient (hours⁻¹)

191

192 With parameter for initial value in the numerical integration:

193 C_0 initial concentration at time $t=0$ (mg TMA-N per 100 g fish)

194

195 The parameter C_0 incorporates the initial freshness status and the effect of natural
196 variation in the quality that influences the freshness of fish and C_{max} was estimated to
197 be 62.2 mg N/100 g cod (Heising et al., 2014c). Since TMA is a metabolite formed by

198 microbial growth, microbiological models and parameter estimations were used to
199 describe the effect of temperature on the formation of TMA on fish. The effect of
200 temperature on the maximum formation rate μ_{max} of the formation of TMA could be
201 described by a model that is analogous to the microbiological extended square root
202 model of Ratkowsky (Ratkowsky, Lowry, McMeekin, Stokes, & Chandler, 1983)
203 (equation 2):

$$204 \mu_{max} = (b(T - T_{min})(1 - \exp^{c(T-T_{max}})))^2 \quad (2)$$

205

206 With:

207 T_{min} minimum temperature at which the rate of TMA formation is zero (°C)

208 T_{max} maximum temperature at which the rate of TMA formation is zero (°C)

209 b regression coefficient (°C h⁻¹)

210 c additional parameter for fit (°C h⁻¹)

211

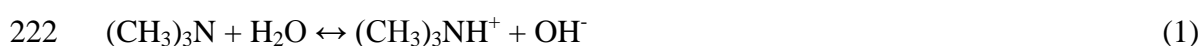
212 The parameter estimate for T_{max} was 25 °C (taken from Dalgaard (1993)) and was
213 based on the maximum growth temperature of the bacteria *Photobacterium*
214 *phosphoreum*. The parameter estimates for the parameters T_{min} , b and c were -4 °C,
215 0.029 °C h⁻¹ and 0.12 °C h⁻¹, respectively (Heising et al., 2014c).

216

217 3.1.2 Dissociation of TMA in fish

218 The TMA that is formed by the micro-organisms will partly dissolve and dissociate in
219 the fish tissue and a part will be present in the free form being able to partition to the
220 headspace of the package. The dissociation reaction of TMA is:

221



223

224 The fraction of the total TMA that is formed (from equation 1, formation model) that
225 remains in the undissociated form can be expressed according to equation 3. The
226 density ρ_f of cod (1.0541 g/ml (Lowndes, 1955)) was used for converting the unit of
227 mg N/100 g fish from equation 1 to the unit of mg/l.

228

$$229 \quad F = \frac{[TMA]}{[\Sigma TMA]} = \frac{[TMA]}{[TMA]+[TMAH^+]} \quad (3)$$

230

231 With:

232 F fraction of TMA in ΣTMA of the fish (-)

233 $[TMA]$ concentration of undissociated TMA (mg l^{-1})

234 $[TMAH^+]$ concentration of dissociated TMA (mg l^{-1})

235 $[\Sigma TMA]$ concentration of total TMA from equation X (mg l^{-1})

236

237 The dissociation equilibrium is described by the dissociation constant, which is
238 expressed as (equation 4):

$$239 \quad K_a = \frac{[TMA][H^+]}{[TMAH^+]} \quad (4)$$

240

241 With:

242 K_a dissociation constant

243 $[H^+]$ concentration of hydrogen ion (mg l^{-1})

244

245 The dissociation constant pK_a ($=-\log K_a$) for TMA at 25 °C is 9.81. The dissociation
246 constant depends on the temperature of the fish. Equation 5 describes the temperature
247 dependence of the pK_a of TMA. This equation was adapted from the temperature

248 dependence of the pK_a of NH_3 (Emerson, Russo, Lund, & Thurston, 1975), assuming
249 the same temperature coefficient for TMA as was reported for NH_3 (Howgate, 2010).

$$250 \quad pK_a = 0.6516 + 2729.2T^{-1} \quad (5)$$

251

252 With:

253 pK_a dissociation constant of TMA

254 T temperature (K)

255

256 The pH of the fish changes during storage, e.g. due to autolytic reactions or dissolving
257 gases. For the modelling and simulations a pH of 6.9 for raw cod fillets was used
258 (Sivertsvik, Rosnes, & Jeksrud, 2004).

259

260 *3.1.3 Partitioning of TMA between the fish and the headspace*

261 When TMA is formed by micro-organisms on the surface of the cod fillets, part of the
262 TMA will be released to the headspace of the fish package. The partitioning between
263 the fish and the headspace is based on the total TMA content that is formed.

264

265 The ratio of volatiles between the fish and the headspace can be described by K_{hf} :

$$266 \quad K_{hf} = \frac{c_f}{c_h} = k_H * RT \quad (6)$$

267 or rewritten to equation 7 (Sander, 1999):

$$268 \quad T * k_H = 12.2 * K_{hf} \quad (7)$$

269

270 With:

271 K_{hf} ratio of concentrations in headspace and fish (-)

272 c_h concentration of TMA in headspace (mg l^{-1})

273 c_f concentration of TMA in fish (mg l^{-1})

274 k_H Henry's Law constant ($\text{mol l}^{-1} \text{atm}^{-1}$)

275 R gas constant ($8.314 \text{ J K}^{-1} \text{ mol}^{-1}$)

276 T temperature (K)

277

278 The Henry's Law constant for TMA between water and gas phase at 25°C is 9.6 (mol
279 $\text{L}^{-1}) \text{ atm}^{-1}$ (Sander, 1999), it was assumed that the effect of dissolved salts in the fish
280 on this constant can be neglected. This value needs to be calculated for the
281 temperature at which the packed fish is stored. The temperature dependence of the
282 Henry constant can be described by the van 't Hoff equation (Equation 8):

$$283 \quad \frac{d \ln k}{d \frac{1}{T}} = - \frac{\Delta H^\ominus}{R} \quad (8)$$

284

285 In integrated form (Equation 9):

$$286 \quad \ln \left(\frac{k_2}{k_1} \right) = \frac{\Delta H^\ominus}{R} \left(\frac{1}{T_1} - \frac{1}{T_2} \right) \quad (9)$$

287

288 With:

289 R gas constant ($8.314 \text{ J K}^{-1} \text{ mol}^{-1}$)

290 T temperature (K)

291 k Henry constant ($\text{mol l}^{-1} \text{atm}^{-1}$)

292 ΔH^\ominus standard enthalpy change (J mol^{-1})

293

294 The value taken for the slope $\frac{d \ln k}{d \frac{1}{T}}$ was 4100 M atm^{-1} (Sander, 1999), assuming the

295 temperature dependence of TMA to be similar to that of NH_3 . After the Henry's law

296 constant has been adjusted for the storage temperature of the fish, equation 6 is used
297 to calculate the ratio K_{hf} of concentration of TMA in the fish and in the headspace.

298

299 3.1.4 Mass transfer coefficient

300 On the surface of the fish that is exposed to the headspace, the release of TMA will
301 take place when there is a driving force if the concentrations of undissociated TMA in
302 the fish and in the headspace are not in equilibrium. The rate of change of TMA
303 concentration in the fish per unit of time (h^{-1}) is described by equation 10:

$$304 \quad V \frac{dc_{TMA}}{dt} = K_L A_f (c_f - c_h) \quad (10)$$

305

306 With:

307 c_{TMA} concentration of dissolved TMA in fish (mg l^{-1})

308 V volume of fish ($=M_f/\rho_f$) ($=0.36 \text{ l}$)

309 K_L mass transfer coefficient (mm h^{-1})

310 A_f surface of fish exposed to headspace ($= 0.02 \text{ m}^2$)

311

312 The mass transfer coefficients of TMA were assumed to be similar to the mass
313 transfer coefficient for NH_3 . Since there is no airflow inside the package, the overall
314 mass transfer rate is mainly dependent on the diffusion coefficient. The diffusion
315 coefficient changes proportionally with the temperature change (according to the
316 Stokes-Einstein equation, the other parameters of the Stokes-Einstein equation were
317 assumed to remain constant in the sensor for the temperature range of 0-15 °C). In the
318 model, the the mass transfer coefficient K_L at temperature T (K) was estimated from
319 $K_{L,\text{ref}}$, using the experimental data (Heising et al., 2014a) at a reference temperature of
320 15 °C (Equation 11).

321 $K_L = K_{Lref} * \frac{T}{T_{ref}}$ (11)

322

323 With:

324 K_L mass transfer coefficient (mm h⁻¹)

325 K_{Lref} reference mass transfer coefficient at 15 °C (mm h⁻¹)

326 T temperature (K)

327 T_{ref} reference temperature (=288 K)

328

329 *3.1.5 Mass transfer of TMA from the headspace to the sensor aqueous phase*

330 The same equations as described above for the mass transfer between the fish and the
331 headspace can be established for the mass transport of TMA from the headspace to
332 the sensing aqueous phase as well. These equations need to be based on the
333 dissociation and partitioning of TMA between the headspace and the sensor aqueous
334 phase, but the dissociation constants and Henry constants are assumed to be similar
335 for the fish and the aqueous phase (but the pH of the sensing aqueous phase is
336 assumed to be 6.0).

337 The mass transfer of TMA in the fish package is schematically shown in figure 2.

338

339 *3.1.6 Sensor measurement*

340 According to the reaction 1 ions are formed when TMA dissolves in the aqueous
341 phase. These ions cause an increase in the conductivity (molar conductivity of TMA
342 is 47.2 S-cm²/mol and that of OH⁻ is 199.1 S-cm²/mol) (Coury, 1999). The molecular
343 weight of TMA of 59.11 g mol⁻¹ was used for converting the unit of mg TMA to the
344 unit moles. The conductivity in the aqueous phase is monitored by the conductivity

345 electrode, from which the TMAH⁺ concentration in the aqueous phase is calculated.
346 From this signal the freshness stage of the fish is predicted.

347

348 *3.1.7 Model equations*

349 The formation and mass transfer of TMA from the fish to the aqueous phase of the
350 sensor is described by differential equations, based on the equations described above.

351 The model equations are based on mass balances, for example the TMA content in the
352 fish is based on the formation of TMA from microbial growth minus the release of
353 TMA from the fish to the headspace. The mass balances are described separately for
354 the TMA in the fish, the headspace and the sensing aqueous phase. Finally, a
355 dissociated TMAH⁺- concentration in the sensing aqueous phase can be calculated at
356 each time t resulting in a conductivity value. This conductivity value represents the
357 freshness status of the fish.

358

359 The differential equations are numerically integrated with the software in order to
360 simulate the TMA content in the fish, the headspace and the sensing aqueous phase.

361 The initial conditions for numerical integration of the differential equations are:

362 U(1) initial concentration of TMA in fish at time 0 = $C_{0*}\rho_f$ (mg l⁻¹)

363 U(2) initial concentration of TMA in headspace at time 0 = 0 (mg l⁻¹)

364 U(3) initial concentration of TMA in aqueous phase at time 0 = 0 (mg l⁻¹)

365 U(4) initial concentration of TMAH⁺ in aqueous phase at time 0 = 0 (mg l⁻¹)

366

367 **3.2 Model application**

368

369 *3.2.1 Fit of the mathematical model on measurements of a fish storage trial*

370 The model was fitted on the measurements of conductivity during a storage trial
371 (Figure 3). The fits of the model and the measurements are quite similar, therefore the
372 general trend of the measurements is confirmed by the model.

373

374 The value for the parameter mass transfer coefficient from the release of TMA from
375 the fish to the headspace was $3.81 \cdot 10^{-3} \pm 2.0 \cdot 10^{-4} \text{ mm} \cdot \text{h}^{-1}$ and from the uptake of
376 TMA from the headspace into the sensing aqueous phase was $6.93 \cdot 10^{-3} \pm 2.7 \cdot 10^{-4}$
377 $\text{mm} \cdot \text{h}^{-1}$ (both values were estimated from least squares regression of the model on the
378 measured data). It was not expected that the release from the fish proceeds slower
379 than the uptake in the sensing aqueous phase, but the parameters are strongly
380 correlated (-0.998) and perhaps the matrix of the fish tissue plays a role in the release
381 of TMA.

382 The mass transfer coefficient is dependent on the dimensions of the system. Since
383 convection does not play a role in the transport of TMA in the package, molecular
384 diffusion is expected to influence the mass transfer coefficient the most (Equation 12):

$$385 \quad K_L = \frac{D}{\delta} \quad (12)$$

386

387 With

388 D diffusion coefficient (m^2/s)

389 δ distance across diffusion occurs (m)

390

391 TMA- H^+ that is dissolved in the fish fillet and is released to the headspace is expected
392 to diffuse over a small distance, since it was assumed that spoilage changes are
393 normally present and most active on the surface of the fish, therefore most TMA will
394 be accumulated at the surface zone (Dyer, Sigurdsson, & Wood, 1944). The estimated

395 mass transfer coefficients for the release of TMA from the fish is in the order of 10^{-9}
396 m/s, which is in the same order as diffusion coefficients for NH_3 reported by Frank,
397 Kuipers, & Van Swaaij (1996), but is expected to be higher because of the low δ .

398

399 The conductivity in the aqueous phase is measured by the sensor, but the conductivity
400 electrode is non-specific and can measure all volatile compounds that dissolve and
401 dissociate in the aqueous phase. Therefore, also other volatile compounds, e.g. NH_3 ,
402 CO_2 , and H_2S that can be formed by the fish can influence the signal that is measured
403 by the sensor. Furthermore, from reaction 1 it can be seen that OH^- ions are formed
404 together with the TMAH^+ . Besides, the compounds can interact with each other, e.g.
405 the carbonic acid from dissolved CO_2 can react with the hydrogen ions formed from
406 the dissociation of trimethylamine in the aqueous phase.

407 Furthermore, the parameter μ_{max} for the formation of TMA at different temperature is
408 estimated from equation 2. Small deviations in this parameter will influence the rate
409 of TMA formation and TMA concentrations in the fish, headspace and aqueous phase
410 strongly. This might influence the predictions for the mass transfer coefficient as well.
411 Despite these drawbacks very characteristic profiles of the electrode signals were
412 observed during various storage trials at temperatures between 0 and 15 °C, which
413 proofs the reliability of this method.

414

415 *3.2.2 Simulations with geometry*

416 Simulations at 0 °C were conducted with the model to study the effect of the
417 geometric parameters. The parameters sensor volume and surface, and headspace
418 volume were varied and compared with the standard laboratory experimental setup
419 (Figure 1), except when other values for geometry parameters are mentioned. The

420 simulation results need to be validated during the future experimental design of the
421 sensors.

422

423 3.2.2.1 Effect of sensor volume and surface

424 In the standard experimental setup the sensor had a large volume of 65 ml with a
425 surface of sensor exposed to headspace of $3.85 \cdot 10^{-3} \text{ m}^2$. To convert this laboratory
426 setup into an intelligent packaging sensor the sensing aqueous phase and electrodes
427 need to be minimized (Vanderroost et al., 2014). Simulations at 0 °C were conducted
428 with the model to study the effect of the geometric parameters. When the volume of
429 the aqueous phase decreases, the surface of the aqueous phase decreases as well. The
430 surface exposed to the headspace depends on the shape of the aqueous phase, however
431 for the simulations we used equation 13 to calculate the surface belonging to the
432 reduced volume.

$$433 \quad A_2 = A_1 \left(\frac{V_2}{V_1} \right)^{2/3} \quad (13)$$

434

435 In the sensor in the laboratory setup, dissolved TMA needs to diffuse over ~10 mm
436 before being measured. When the geometry of the sensor changes, this diffusion
437 distance will change as well. To take this effect on the mass transfer coefficient of the
438 sensor uptake into account in the simulations, the mass transfer coefficient was
439 corrected according to equation 14:

$$440 \quad K_{L2} = K_{L1} \left(\frac{V_2}{V_1} \right)^{1/3} \quad (14)$$

441

442 When the volume of the aqueous phase is reduced, the concentration of TMA in the
443 aqueous phase increases (Figure 4). This increased TMAH⁺ concentration in the

444 aqueous phase will increase the sensitivity of the sensor response to different stages of
445 freshness. So when minimizing the sensor, the signal will be optimized as well.

446

447 3.2.2.2 Effect of headspace volume

448 In the non-destructive setup in the laboratory, a glass cell with a large volume (1.6 L)
449 compared to the mass of the packed fish (0.375 kg) was used. A ratio between the
450 volume of a gas and volume of food product (G/P ratio) in a modified atmosphere
451 packaging for cod is usually 2:1 or 3:1 (Sivertsvik, Jeksrud, & Rosnes, 2002). In the
452 simulations the volume of the headspace was varied from a ratio of 1:1 until 3:1 and
453 compared with the laboratory experimental setup (4.3:1). In the simulations a volume
454 of 0.1 ml and surface of $5.13 \cdot 10^{-5}$ were taken as values to simulate the parameters of
455 a minimized sensor. From figure 5 it can be seen that the signal of the electrode will
456 increase when the headspace volume is decreased, therefore the sensor sensitivity will
457 improve when the concept is applied on a package with a regular volume, but it will
458 only be a small effect.

459

460

461 *3.2.3 Simulations with variation in initial freshness on the prediction of freshness*

462 *in the supply chain*

463 TMA is produced on fresh cod fillets stored at chilled temperatures by micro-
464 organisms. The species and number of microorganisms on fish on the moment of
465 catch varies greatly; A normal range of 10^2 - 10^7 cfu/cm² on the skin surface and
466 between 10^3 and 10^9 cfu/g on both the gills and the intestines have been reported
467 (Huss, 1995). This variability is influenced by (partially) uncontrollable factors, like
468 season and environmental conditions (e.g. pollution, temperature) of place of catch

469 (Gram & Huss, 1996). Besides, the time and temperature between catch and moment
470 of packaging varies, resulting in differences in the initial freshness status of the fish
471 fillets. The initial freshness is incorporated in the model of the formation of TMA in
472 the value of parameter C_0 , which is the initial TMA concentration (mg l^{-1}) in the
473 packed fish. The effect of natural variation in the initial freshness status was simulated
474 using different values for the parameter C_0 (Figure 6), the range of the values for C_0
475 taken from parameter estimations from real trials from Heising et al., 2014c. To
476 simulate minimized sensor conditions a volume of 0.1 ml and surface of $5.13 \cdot 10^{-5}$
477 were taken and the headspace volume was set on 750 ml (G/P ratio 2:1). A higher C_0
478 will lead to a faster increase in the sensing aqueous phase. But the simulations also
479 show that the initial freshness status does have a large impact on the freshness
480 predictions at advanced storage times since the concentrations still increase
481 exponentially.

482

483

484 *3.2.4 Simulations with dynamic temperatures on the prediction of freshness in the* 485 *supply chain*

486 In the simulations above the temperature was set at 0 °C. Figure 7 shows that
487 according to simulations with other temperatures (with other parameters set for a
488 miniaturized sensor), the dissociated TMA in the sensing aqueous phase increases
489 strongly with increasing storage temperature.

490

491 However, the temperature fluctuates in the cod supply chain (Haflidason, Ólafsdóttir,
492 Bogason, & Stefánsson, 2012). A chain with temperature abuse was simulated: In a
493 simulation (with a sensor with miniaturized conditions) fish was stored at 0 °C, but

494 after 100 hours, the temperature increased to 15 °C for 10 hours, and then returned to
495 0 °C. The temperature abuse is clearly seen in a sudden fast increase in the TMA
496 concentration in the packed fish (Figure 8A). This sudden increase is not seen directly
497 in the aqueous phase, but after the temperature abuse the concentration of dissociated
498 TMA in the sensing aqueous phase is considerably higher compared to the simulation
499 at constant 0 °C (Figure 8B).

500

501

502 *3.2.5 Practical considerations to translate the predicted sensor outcome to a*
503 *freshness signal*

504 The non-destructive method has potential to be developed into an intelligent
505 packaging. Taken this in perspective, the predicted sensor signal needs to be
506 translated into a freshness signal that can be communicated as freshness status of the
507 packed fish.

508 Although a level of 30 mg TMA 100 g⁻¹ has been found at rejection level for packed
509 cod (Dalgaard, 1995), the spoilage level was set to the acceptability limit for chilled
510 cod of 15 mg TMA 100 g⁻¹ reported by Venugopal, 2002 to calculate the moment of
511 spoilage according to the sensor predictions (this acceptability limit is taken to
512 illustrate the principle, every other TMA value can be taken as well). However,
513 different TMA acceptability limits have been reported in literature, since this depends
514 on the definition of the rejection point that is regarded as unacceptable (e.g. Dalgaard,
515 Gram, & Huss (1993) found a level of >30 mg TMA 100 g⁻¹ as rejection point, but the
516 rejection point was defined as the point when 50% of the panelists rejected the fillets,
517 which might not be realistic in commercial practice).

518 Simulations where performed with the miniaturized parameter conditions, the
519 temperature and initial TMA concentration in the fish were varied for the simulations
520 of different scenarios. The freshness predictions based on the TMA content of the fish
521 were compared to the model prediction of the content of TMAH⁺ in the aqueous
522 phase.

523 At a constant temperature of 0 °C, the spoilage limit of 15 mg N TMA 100 g⁻¹ fish
524 was reached after 387 h. At this time, the TMAH⁺ in the sensing aqueous phase was
525 0.0552 mg l⁻¹ (Table 1). In the temperature abuse simulation (fish stored at 0 °C, the
526 temperature increases to 15 °C for 10 hours after 100 hours, then returns back to 0 °C
527 for remaining time) the fish reached the spoilage limit after 278 hours, which is more
528 than 100 hours earlier compared to the simulation at a constant temperature of 0 °C.

529 At 278 hours the TMAH⁺ concentration in the sensing aqueous phase is 0.0503 mg l⁻¹,
530 the TMAH⁺ concentration of 0.0552 mg l⁻¹ (comparable to TMAH⁺ concentration in
531 aqueous phase at spoilage moment at 0 °C constant) is reached after 286 hours. If one
532 would base the spoilage limit on 0.055 mg l⁻¹ in the aqueous phase, this would give a
533 difference in the remaining shelf life of 8 hours.

534 The sensor should also give accurate predictions with different initial TMA
535 concentrations C_0 . A higher initial TMA concentration will lead to a shorter remaining
536 shelf life. When the initial TMA concentration was increased in the simulation from
537 1.53 mg l⁻¹ to 3 mg l⁻¹ the fish reached the spoilage limit of 0.055 mg l⁻¹ in the
538 aqueous phase after 334 hours. At this time also the spoilage limit of 15 mg N TMA
539 100 g⁻¹ fish in the packed fish was reached. This shows that the sensor is able to give
540 accurate freshness predictions with a variable initial freshness status.

541

542 When a simulation was conducted at a constant 4 °C storage temperature, the fish
543 would reach the spoilage limit after 142.3 hours. But the TMAH⁺ concentration in the
544 aqueous phase is only 0.015 mg l⁻¹. The TMAH⁺ concentration of 0.0552 mg l⁻¹ is
545 reached after 269 h when the fish is far beyond spoilage. This implies that the
546 freshness of the fish cannot be estimated solely from the sensor signal in the aqueous
547 phase. Also information on the storage temperature is necessary to determine the cut-
548 off point.

549

550 So the sensor signal at higher temperatures can still be translated into a freshness
551 status of the fish, but the sensor needs to be combined with a temperature sensor.
552 When the sensor signal is combined with the temperature history the model can be
553 used to calculate the initial freshness C_0 and from here a remaining shelf life can be
554 predicted.

555 The simulation results can be used in the future experimental design of the sensors,
556 during this development the results need to be validated.

557

558 **4. Conclusions**

559 This manuscript presents the framework for a mathematical model that describes the
560 mass transport of TMA that is formed on packed fish, released in the headspace and
561 dissolves and dissociates in the sensing aqueous phase. This model is necessary to
562 predict the freshness of the packed fish from the data produced by a non-destructive
563 sensor that monitors TMA in the sensing aqueous phase.

564 The model predicts an TMA increase in the sensing aqueous phase comparable with
565 sensor measurements from a storage trial at 15 °C. Model outcomes from simulations
566 with variation of the sensor geometry show that minimizing the sensing aqueous

567 phase and the package headspace will improve the sensitivity of the sensor to different
568 freshness stages.

569 The model can make accurate freshness predictions at a constant temperature of 0 °C
570 and also in case of temporarily temperature abuse. The initial freshness of fish is
571 variable, the model can be used to estimate it based on the data and use this parameter
572 in the predictions of the freshness status of the packed fish. At 4 °C and higher, the
573 freshness of the packed fish can be estimated when the temperature history is also
574 measured. For variable storage temperatures, the conductivity-sensor has to be
575 combined with a temperature sensor in order to use this model for the development of
576 an intelligent packaging to monitor the freshness of fish.

577

578 **Acknowledgement**

579 This research is financially supported by the Wageningen University Graduate School
580 VLAG and the Dutch Ministry of Agriculture, Nature and Food Quality (KB
581 030013121).

582

583 **References**

584 Botta, J.R., Lauder, J.T., & Jewer, M.A. (1984). Effects of methodology on total
585 volatile basic nitrogen (TVB-N) determination as an index of quality of fresh
586 Atlantic cod (*Gadus morhua*). *Journal of Food Science*, 49, 734-736, 750.

587 Burt, J.R., Gibson, D.M., Jason, A.C., & Sanders, H.R. (1976). Comparison of
588 methods of freshness assessment of wet fish II. Instrumental and chemical
589 assessments of boxed experimental fish. *Journal of Food Technology*, 11, 73-
590 89.

591 Coury, L. (1999). Conductance measurements part 1: Theory. *Current Separations*,
592 18, 91-96.

593 Dalgaard, P. (1993). *Evaluation and prediction of microbial fish spoilage*. Ph.D.
594 Thesis. The Technological Laboratory of the Danish Ministry of Fisheries and
595 the Royal Veterinary and Agricultural University, Copenhagen, Denmark.
596 pp.143.

597 Dalgaard, P., Gram, L., Huss, H.H. (1993). Spoilage and shelf-life of cod fillets
598 packed in vacuum or modified atmospheres. *International Journal of Food*
599 *Microbiology*, 19, 283-294.

600 Dalgaard, P. (1995). Qualitative and quantitative characterization of spoilage bacteria
601 from packed fish. *International Journal of Food Microbiology*, 26, 319-333.

602 Dyer, W.J., Sigurdsson, G.J., & Wood, A.J. (1944). A rapid test for detection of
603 spoilage in sea fish. *Journal of Food Science*, 9, 183-187.

604 Emerson, K., Russo, R.C., Lund, R.E., & Thurston, R.V. (1975). Aqueous ammonia
605 equilibrium calculations: Effect of pH and temperature. *Journal of the Fisheries*
606 *Research Board of Canada*, 32, 2379-2383.

607 Frank, M.J.W., Kuipers, J.A.M., & Van Swaij, W.P.M. (1996). Diffusion
608 coefficients and viscosities of CO₂ + H₂O, CO₂ + CH₃OH, NH₃ + H₂O, and
609 NH₃ + CH₃OH liquid mixtures. *Journal of Chemical and Engineering Data*,
610 41, 297-302.

611 Gill, T.A. (1990). Objective analysis of seafood quality. *Food Reviews International*,
612 6, 681-714.

613 Gram, L. & Huss, H. H. (1996). Microbiological spoilage of fish and fish products.
614 *International Journal of Food Microbiology*, 33, 121-137.

615 Haflíðason, T., Ólafsdóttir, G. Bogason, S., & Stefánsson, G. (2012). Criteria for
616 temperature alerts in cod supply chains. *International Journal of Physical*
617 *Distribution & Logistics Management*, 42, 355-371.

618 Heising, J.K., Dekker, M., Bartels, P.V., & Van Boekel, M.A.J.S. (2012). A non-
619 destructive ammonium detection method as indicator for freshness for packed
620 fish: Application on cod. *Journal of Food Engineering*, 110, 254-261.

621 Heising, J.K., Bartels, P.V., Van Boekel, M.A.J.S., & Dekker, M. (2014a). Non-
622 destructive sensing of the freshness of packed cod fish using conductivity and
623 pH electrodes. *Journal of Food Engineering*, 124, 80-85.

624 Heising, J.K., Dekker, M., Bartels, P.V., & Van Boekel M.A.J.S. (2014b). Monitoring
625 the quality of perishable foods: opportunities for intelligent packaging.
626 *Critical Reviews in Food Science and Nutrition*, 54, 645-654.

627 Heising, J.K., Van Boekel, M.A.J.S., & Dekker, M. (2014c). Mathematical models for
628 the trimethylamine (TMA) formation on packed cod fish fillets at different
629 temperatures. *Food Research International*, 56, 272-278.

630 Howgate, P. (2010). A critical review of total volatile bases and trimethylamine as
631 indices of freshness of fish. Part 1. Determination. *Electronic Journal of*
632 *Environmental, Agricultural and Food Chemistry*, 9, 29-57.

633 Huss, H. H. (1995). Quality and quality changes in fresh fish. FAO Fisheries
634 Technical paper no. 348. FAO, Rome, Italy.

635 Kuswandi, B., Wicaksono, Y., Jayus, Abdullah, A., Heng, L.Y., & Ahmad, M. (2011).
636 Smart packaging: sensors for monitoring of food quality and safety. [*Sensing*](#)
637 [*and Instrumentation for Food Quality and Safety*](#), 5, 137-146.

638 Lowndes, A.G. (1955). Density of fishes – some notes on the swimming of fish to be
639 correlated with density, sinking factor and load carried. *The Annals and*
640 *Magazine of Natural History*, 8, 241-256.

641 Malle, P. & Tao, S.H. (1987). Rapid quantitative determination of trimethylamine
642 using steam distillation. *Journal of Food Protection*, 50, 756-760.

643 Ólafsdóttir, G., Martinsdóttir, E., Oehlenschläger, J., Dalgaard, P., Jensen, B.,
644 Undeland, I., Mackie, I. M., Henehan, G., Nielsen, J., & Nilsen, H. (1997).
645 Methods to evaluate fish freshness in research and industry. *Trends in Food*
646 *Science and Technology*, 8, 258-265.

647 Ratkowsky, D.A., Lowry, R.K., McMeekin, T.A., Stokes, A.N., & Chandler, R.E.
648 (1983). Model for bacterial culture growth rate throughout the entire biokinetic
649 temperature range. *Journal of Bacteriology*, 154, 1222-1226.

650 Realini, C.E. & Marcos, B. (2014). Active and intelligent packaging systems for a
651 modern society. *Meat Science*, 98, 404-419.

652 Sander, R. (1999). Compilation of Henry's law constants for inorganic and organic
653 species of potential importance in environmental chemistry. Version 3.
654 Unpublished manuscript. 107 pp. <http://www.henrys-law.org> (accessed on 2
655 October, 2013).

656 Sivertsvik, M., Jeksrud, W.K., & Rosnes, J.T. (2002). A review of modified
657 atmosphere packaging of fish and fishery products – significance of microbial
658 growth, activities and safety. *International Journal of Food Science and*
659 *Technology*, 37, 107-127.

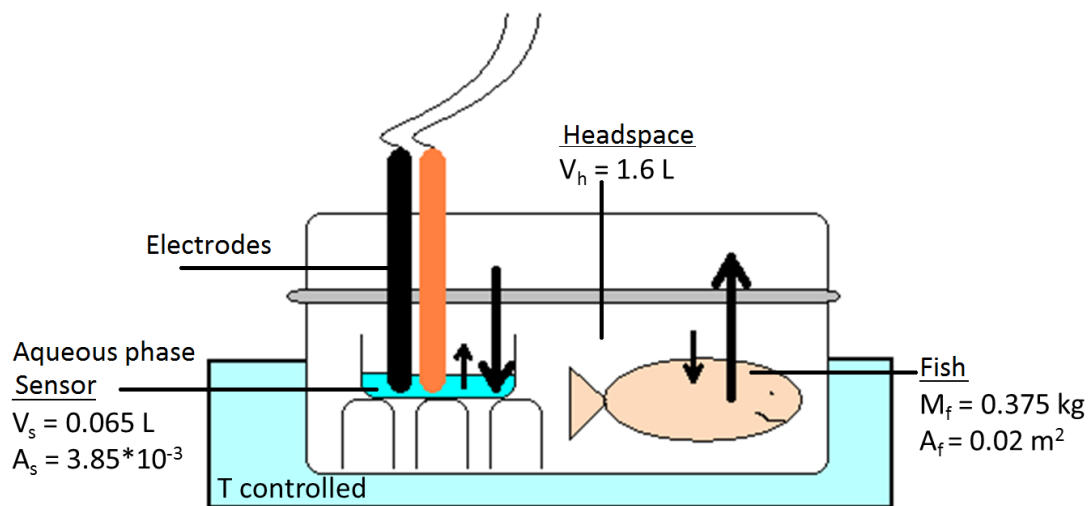
660 Sivertsvik, M., Rosnes, J.T., & Jeksrud, W.K. (2004). Solubility and absorption rate
661 of carbon dioxide into non-respiring foods. Part 2: Raw fish fillets. *Journal of*
662 *Food Engineering*, 63, 451-458.

663 Stewart, W. E., Caracotsios, M., & Sorensen, J. P. (1992). Parameter-estimation from
664 multiresponse data. *AIChE Journal*, 38(5), 641-650.

665 Vanderroost, M., Ragaert, P., Devlieghere, F., & De Meulenaer, B. (2014). Intelligent
666 food packaging: The next generation. *Trends in Food Science & Technology*,
667 39, 47-62.

668 Venugopal, V. (2002). Biosensors in fish production and quality control. *Biosensors*
669 *and Bioelectronics*, 17, 147-157.

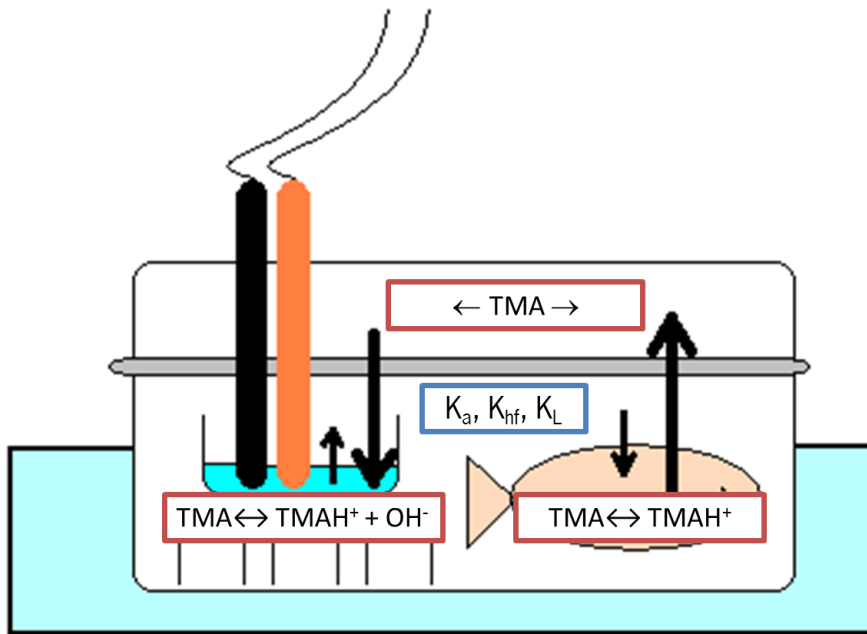
670



671

672 *Figure 1: Systematic picture of the measurement set-up with geometric parameter*
 673 *values ($M = \text{mass}$, $V = \text{Volume}$, $A = \text{Surface}$, $T = \text{Temperature}$) of fish (subscript f),*
 674 *headspace (subscript h) and sensor (subscript s).*

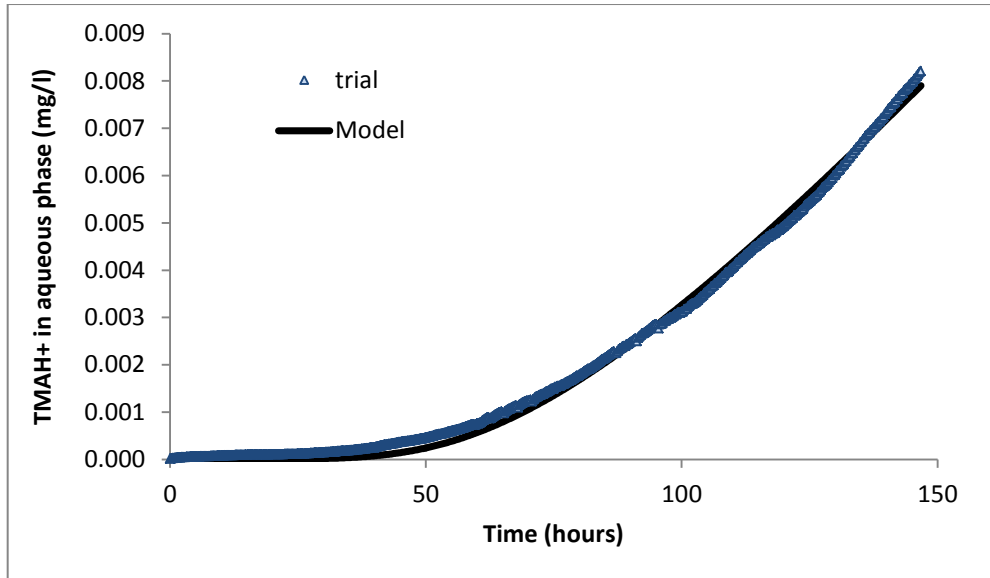
675



676

677 *Figure 2: Schematic picture of mass transfer of TMA in the fish package*

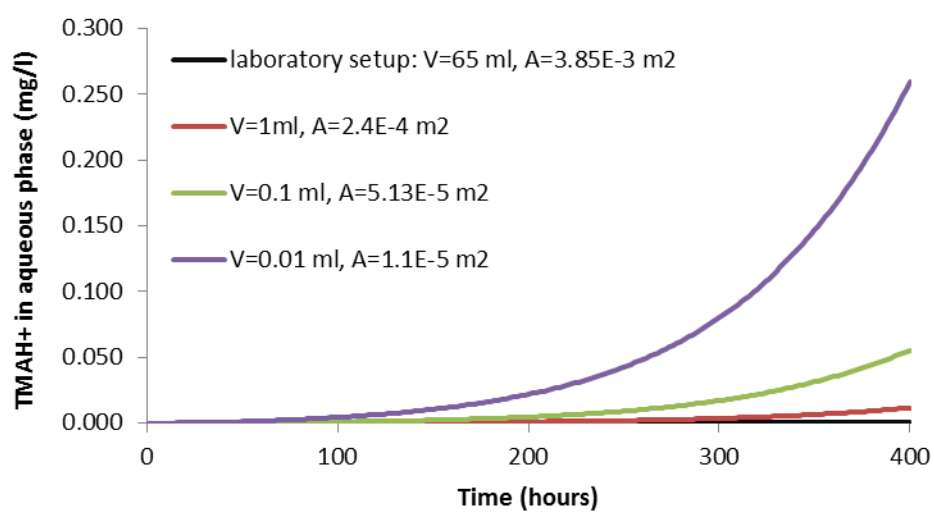
678



679

680 *Figure 3: Fit of the model on sensor measurements of TMAH⁺-concentration from a*
681 *storage trial with cod stored at 15 °C.*

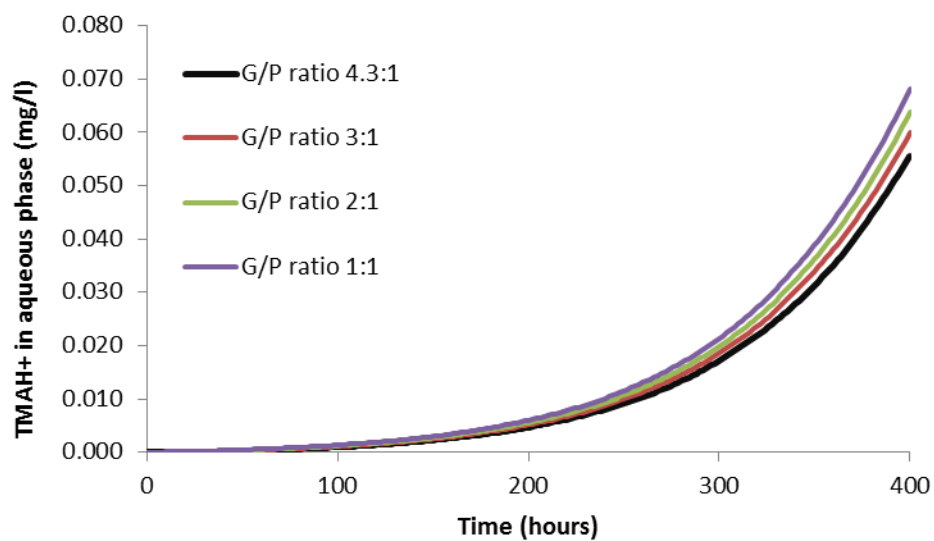
682



683

684 *Figure 4: Effect of volume and surface of sensor exposed to headspace (with*
 685 *corrected K_L) on the concentration of TMA (mg/l) in the sensing aqueous phase from*
 686 *simulations at 0 °C.*

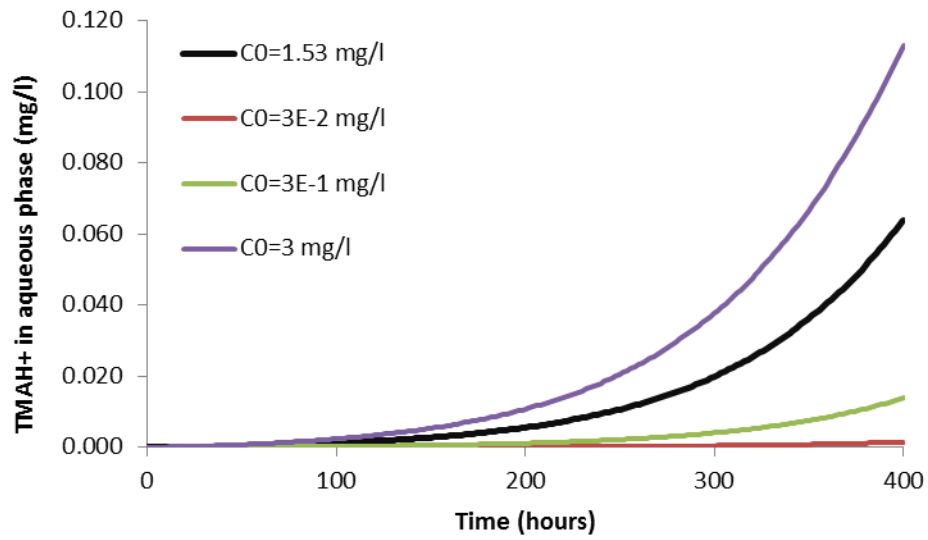
687



688

689 *Figure 5: Effect of headspace volume on the concentration of TMAH⁺ in the sensing*
 690 *aqueous phase from simulations at 0 °C ($V_s=0.1$ ml; $A_s=5.13 \cdot 10^{-5}$).*

691

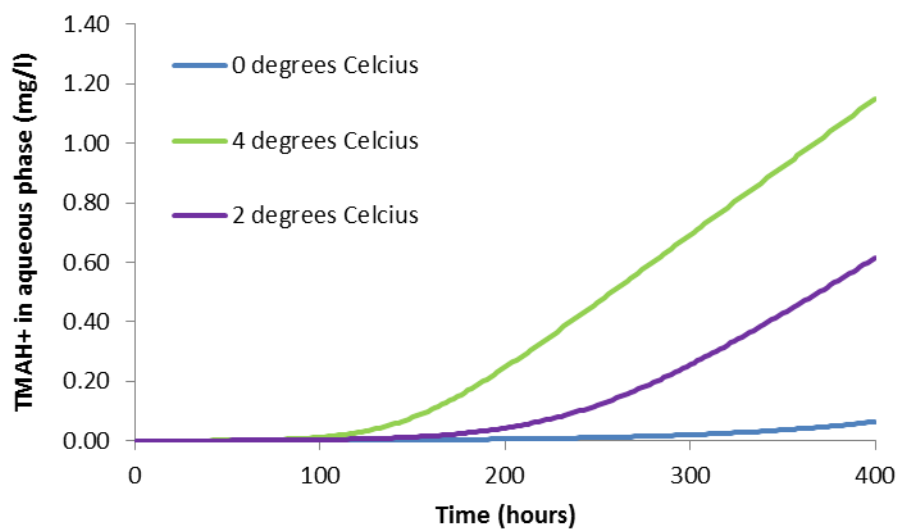


692

693 *Figure 6: Effect of parameter C_0 on the concentration of $TMAH^+$ in the sensing*
 694 *aqueous phase from simulations at 0 °C ($V_s=0.1$ ml; $A_s=5.13 \cdot 10^{-5}$; $V_h=750$ ml).*

695

696



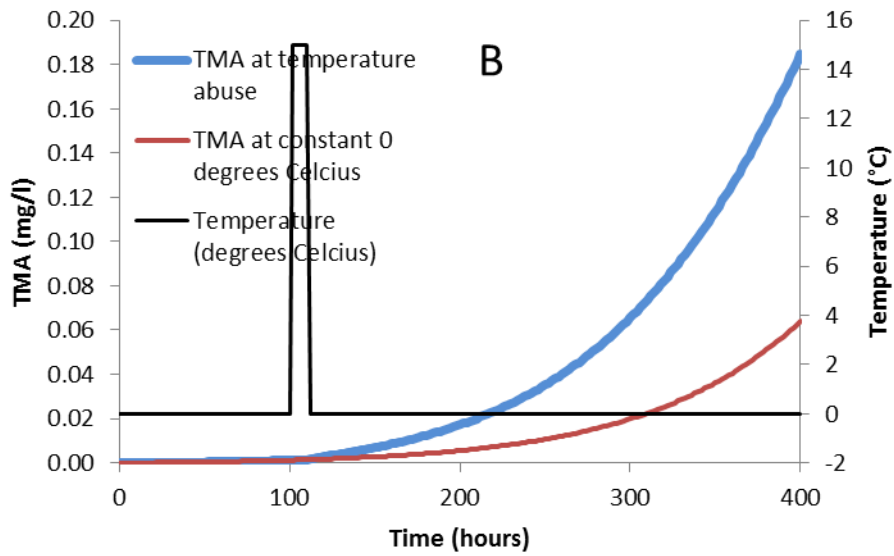
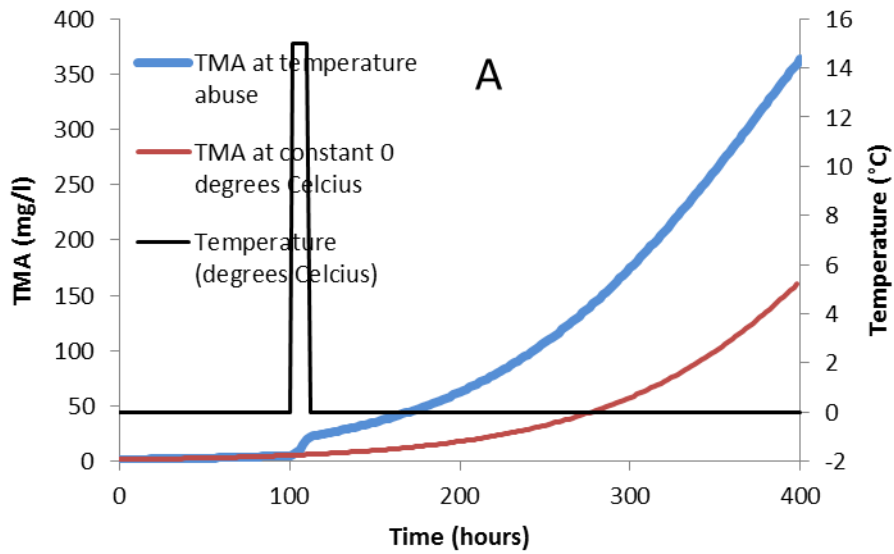
697

698 *Figure 7: Effect of storage temperature on the concentration of TMAH⁺ in the sensing*
699 *aqueous phase from simulations at 0, 2 and 4 °C ($V_s=0.1$ ml; $A_s=5.13 \cdot 10^{-5}$; $V_h=750$*
700 *ml).*

701

702

703



704

705 *Figure 8: Effect of abuse temperature on the concentration of TMA in the packed fish*

706 *(A) and of TMAH⁺ in the sensing aqueous phase (B) from a simulation at 0 °C except*

707 *for 10 hours at 15 °C compared to a simulations with a constant T of 0 °C ($V_s=0.1$*

708 *ml; $A_s=5.13 \cdot 10^{-5}$; $V_h=750$ ml).*

709

710 *Table 1: Results of the simulations of the different scenarios, with varying*
 711 *temperature and initial content: Time when fish is spoiled, corresponding content of*
 712 *TMA in packed fish, and corresponding sensor signal TMAH⁺ in aqueous phase*
 713 *(simulations performed with miniaturized sensor conditions: $V_s=0.1$ ml; $A_s=5.13*10^{-5}$;*
 714 *$V_h=750$ ml)*

Simulation T	Time (hours)	TMA in packed fish (mg l ⁻¹)	TMAH ⁺ in aqueous phase (mg l ⁻¹)
0 °C constant	387	142.3	0.0552
T abuse	278	142.3	0.0503
	286	153.3	0.0552
4 °C constant	105	142.3	0.015
	269	654.4	0.0552
$C_0 = 3$ mg l ⁻¹	334	144.4	0.0552

715

716